Journal of
Mechanical
Science and
Technology

Journal of Mechanical Science and Technology 21 (2007) 678~689

Two-Phase Non-Linear Model for the Flow Through Stenosed Blood Vessels

D. S. Sankar[a], Usik Lee[a,*]

[a]*Department of Mechanical Engineering, Inha University 253 Yonghyun-Dong, Nam-Gu, Incheon 402-751, Korea (Currently on leave from Department of Mathematics, Crescent Engineering College Vandalur, Chennai–600 048, Tamil Nadu, India)*

(Manuscript Received October 17, 2006; Revised February 5, 2007; Accepted February 6, 2007)

Abstract

Pulsatile flow of a two-phase model for blood flow through arterial stenosis is analyzed through a mathematical analysis. The effects of pulsatility, stenosis, peripheral layer and non-Newtonian behavior of blood, assuming the blood in the core region as a Herschel-Bulkley fluid and the plasma in the peripheral layer as a Newtonian fluid, are discussed. A perturbation method is used to solve the resulting system of non-linear quasi-steady differential equations. The expressions for velocity, wall shear stress, plug core radius, flow rate and resistance to flow are obtained. It is noticed that the plug core radius and resistance to flow increase as the stenosis size increases while all other parameters held constant. The wall shear stress increases with the increase of yield stress while keeping other parameters as invariables. It is observed that the velocity increases with the axial distance in the stenosed region of the tube upto the maximum projection of the stenosis.

Keywords: Two-phase model; Non-newtonian fluid; Newtonian fluid; Pulsatile flow; Stenosed blood vessel

1. Introduction

Blood flow characteristics in arteries can be altered significantly by arterial disease, such as stenosis and aneurysm. The development of arteriosclerosis in blood vessels is quite common which may be attributed to the accumulation of lipids in the arterial wall or pathological changes in the tissue structure (Liepsch et al., 1992). Arteries are narrowed by the development of atherosclerotic plaques that protrude into the lumen, resulting in stenosed arteries. When an obstruction is developed in an artery, one of the most serious consequences is the increased resistance and the associated reduction of the blood flow to the particular vascular bed supplied by the artery. Thus, the presence of a stenosis can lead to the serious circulatory disorder.

Recently several theoretical and experimental investigations have been performed to study the blood flow characteristics due to the presence of a stenosis in the arterial lumen of a blood vessel (Sankar and Hemalatha, 2006; Mandal, 2005; Marshall, 2004; Moayeri and Zendehbudi, 2003; Liu et al., 2004; Bakirtas and Antar, 2003; Long et al., 2001; Segers and Verdonck, 2000). Since, the blood flow through narrow arteries is highly pulsatile, more attempts have been made to study the pulsatile flow of blood treating blood as a Newtonian fluid (Long et al., 2001; Dash et al., 1999; Moayeri and Zendehbudi, 2003; Liu et al., 2004; Chakravarthy and Mandal, 2000). The Newtonian behavior may be true in larger arteries, but, blood, being a suspension of cells in plasma, exhibits non–Newtonian behavior at low

*Corresponding author. Tel.: +82 32 860 7318, Fax.: +82 32 866 1434
E-mail address: ulee@inha.ac.kr

shear rates $(\dot{\gamma} < 10/\sec)$ in small diameter arteries (0.02 mm–0.1 mm), particularly, in diseased state, the actual flow is distinctly pulsatile (Sankar and Hemalatha, 2006; Liu et al., 2004; Chaturani and Ponnalagar Samy, 1986). Several researchers have analyzed the non–Newtonian behavior and pulsatile flow of blood through stenosed arteries (Sankar and Hemalatha, 2006; Mandal, 2005; Tu and Deville, 1996; Chaturani and Ponnalagar Samy, 1985; 1986).

Bugliarello and Sevilla (1970) and Cokelet (1972) have reported that for blood flowing through narrow blood vessels, there is a peripheral layer of plasma (Newtonian fluid) and a core region of suspension of all the red cells as a non-Newtonian fluid. Their experimentally measured velocity profiles in the narrow arteries confirm the impossibility of representing the velocity distribution by a single-fluid model which ignores the presence of the peripheral layer that plays a crucial role in determining the flow patterns of the system. Thus, for a realistic description of blood flow, perhaps, it is more appropriate to treat blood as a two-fluid model. Several researchers have studied the two-phase models for blood flow through stenosed arteries treating the fluid in the core region as a non-Newtonian fluid and the fluid in the peripheral layer as a Newtonian fluid (Srivastava and Saxena, 1994; Srivastava, 1996; Pralhad and Schultz, 1988; Shukla et al., 1980a, 1980b). Srivastava and Saxena (1994) have studied a two-phase model for blood flow through stenosed arteries assuming the fluid in the core region as a Casson fluid and the plasma in the peripheral layer as a Newtonian fluid. In the present model, we study a two-phase model for pulsatile flow of blood through stenosed narrow arteries (of diameter 0.02 – 0.1mm) at low shear rates $(\dot{\gamma} < 10/\sec)$, assuming the fluid in the core region as a Herschel-Bulkley (H-B) fluid while the fluid in the peripheral region as a Newtonian fluid.

The suspension of all the erythrocytes in the core region of the blood flow behaves like a non-Newtonian fluid (Srivastava and Saxena, 1994). Kapur (1992) reported that Herschel-Bulkley and Casson fluid models are suitable to represent blood when it flows through narrow arteries at low shear rates. Chaturani and Ponnalagar Samy (1985) have mentioned for tube diameter 0.095 mm, blood behaves like Herschel-Bulkley fluid rather than power law and Bingham fluids. Iida (1978) reports "The velocity profiles in the arterioles having diameter less than 0.1 mm are generally explained fairly by the Casson and Herschel-Bulkley fluid models. However, the velocity profiles in the arterioles whose diameters less than 0.0650 mm do not conform to the Casson fluid model, but, can still be explained by the Herschel–Bulkley model". Since, the Herschel-Bulkley fluid model can be reduced to the Newtonian fluid model, power law fluid model and Bingham fluid model for appropriate values of the power law index (n) and yield index ($\bar{\tau}_y$), it is possible to study the two-phase fluid models of power law fluid, Bingham fluid and Newtonian fluid from the present analysis. Furthermore, Herschel-Bulkley fluid's constitutive equation has one more parameter namely the power law index (n) than the Casson fluid, one can obtain more detailed information about the flow characteristics by treating the fluid in the core region as a Herschel-Bulkley fluid rather than Casson fluid (Iida, 1978). Hence, we felt that it is appropriate to represent the fluid in the core region of the two-fluid model by the Herschel–Bulkley fluid model rather than the Casson fluid model.

Thus, in this paper, we study a two-phase model for blood flow through narrow arteries (of diameter 0.02 mm–0.1 mm) with mild stenosed at low shear rates $(\dot{\gamma} < 10/\sec)$ treating the fluid in the core region as a Herschel-Bulkley fluid and the plasma in the peripheral region as a Newtonian fluid.

2. Mathematical formulation

Consider an axially symmetric, laminar, pulsatile and fully developed flow of blood (assumed to be incompressible) in the $\bar{z}$ (axial) direction through a circular artery with an axially symmetric mild stenosis. It is assumed that the walls of the artery are rigid and the blood is represented by a two-fluid model with a core region of suspension of all erythrocytes as a Herschel-Bulkley fluid and a peripheral layer of plasma as a Newtonian fluid. The geometry of the arterial stenosis is shown in Fig. 1. We have used the cylindrical polar coordinates $(\bar{r}, \bar{\phi}, \bar{z})$. It can be shown that the radial velocity is negligibly small and can be neglected for a low Reynolds number flow in a tube with mild stenosis. In this case, the basic momentum equations governing the flow and the constitutive equations in non-dimensional form are

$$\alpha_H{}^2 \frac{\partial u_H}{\partial t} = 4q(z) f(t) - \frac{2}{r}\frac{\partial}{\partial r}(r\tau_H) \quad \text{if} \quad 0 \le r \le R_1(z) \tag{1}$$

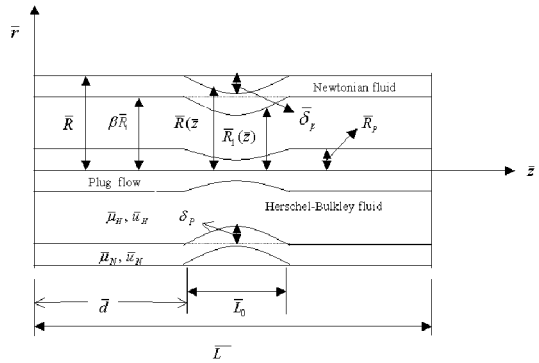

Fig. 1. Two-phase model for the blood flow through a stenosed artery.

$$\alpha_N^{\,2}\frac{\partial u_N}{\partial t}=4q(z)f(t)-\frac{2}{r}\frac{\partial}{\partial r}(r\tau_N) \quad \text{if} \quad R_1(z)\le r\le R(z) \tag{2}$$

$$\tau_H=\sqrt{-\frac{1}{2}\frac{\partial u_H}{\partial r}}+\theta \quad \text{if } \tau_H\ge\theta \text{ and } R_p\le r\le R_1(z) \tag{3}$$

$$\frac{\partial u_H}{\partial r}=0 \quad \text{if} \quad \tau_H\le\theta \quad \text{and} \quad 0\le r\le R_p \tag{4}$$

$$\tau_N=-\frac{1}{2}\frac{\partial u_N}{\partial r} \quad \text{if} \quad R_1(z)\le r\le R(z) \tag{5}$$

where $f(t) = 1 + A \sin t$; u_H and u_N are the fluid velocities in the core region and in the peripheral region, respectively; τ_H and τ_N are the shear stresses for the Herschel-Bulkley fluid and Newtonian fluid respectively; α_H and α_N are the pulsatile Reynolds numbers of the Herschel-Bulkley fluid and Newtonian fluid, respectively. The boundary conditions (in dimensionless form) are

$$\begin{aligned}&\tau_H \text{ is finite and } \frac{\partial u_H}{\partial r}=0 \text{ at } r=0,\\ &u_N=0 \text{ at } r=R(z)\\ &\tau_H=\tau_N,\ u_H=u_N \text{ at } r=R_1(z)\end{aligned} \tag{6}$$

The geometry of the stenosis in the peripheral region (in dimensionless form) is given by

$$R(z)=\begin{cases}1 & \text{in the normal artery region}\\ 1-\dfrac{\delta_p}{2}\left[1+\cos\dfrac{2\pi}{L_0}\left(z-d-\dfrac{L_0}{2}\right)\right] & \text{in } d\le z\le d+L_0\end{cases} \tag{7}$$

The geometry of the stenosis in the core region (in dimensionless form) is given by

$$R_1(z)=\begin{cases}\beta & \text{in the normal artery region}\\ \beta-\dfrac{\delta_C}{2}\left[1+\cos\dfrac{2\pi}{L_0}\left(z-d-\dfrac{L_0}{2}\right)\right] & \text{in } d\le z\le d+L_0\end{cases} \tag{8}$$

The non-dimensional volume flow rate Q is given by

$$Q=4\int_0^{R(z)}u(r,z,t)\,r\,dr \tag{9}$$

The following non-dimensional variables are used to get Eqs. (1)~(9).

$$\begin{aligned}&z=\frac{\bar z}{\bar R_0},\ R(z)=\frac{\bar R(\bar z)}{\bar R_0},\ R_1(z)=\frac{\bar R_1(\bar z)}{\bar R_0},\ r=\frac{\bar r}{\bar R_0},\\ &t=\bar\omega\bar t,\ d=\frac{\bar d}{\bar R_0},\ L_0=\frac{\bar L_0}{\bar R_0}\ q(z)=\frac{\bar q(\bar z)}{\bar q_0}\\ &u_H=\frac{\bar u_H}{\dfrac{\bar q_0\ \bar R_0^{\,2}}{4\bar\mu_0}},\ u_N=\frac{\bar u_N}{\dfrac{\bar q_0\ \bar R_0^{\,2}}{4\bar\mu_N}},\ \tau_H=\frac{\bar\tau_H}{\dfrac{\bar q_0\ \bar R_0}{2}},\\ &\tau_N=\frac{\bar\tau_N}{\dfrac{\bar q_0\ \bar R_0}{2}},\ \theta=\frac{\bar\tau_y}{\dfrac{\bar q_0\ \bar R_0}{2}},\ \alpha_H^{\,2}=\frac{\bar R_0^{\,2}\bar\omega\bar\rho_H}{\bar\mu_0}\\ &\alpha_N^{\,2}=\frac{\bar R_0^{\,2}\ \bar\omega\bar\rho_N}{\bar\mu_N},\ R_p=\frac{\bar R_p}{\bar R_0},\ \delta_p=\frac{\bar\delta_p}{\bar R_0},\ \delta_C=\frac{\bar\delta_C}{\bar R_0},\\ &Q\ =\ \bar Q\Big/\left[\pi\bar R_0^4\bar q_0/8\bar\mu_0\right],\ -\frac{\partial\bar p}{\partial\bar z}\ =\ \bar q(\bar z)f(\bar t)\end{aligned} \tag{10}$$

where $\bar R(\bar z)$ is the radius of the artery in the stenosed peripheral region, R_0' is the radius of the normal artery, L_0' is the length of the stenosis, d' indicates its location and $\bar\delta_p$ is the maximum height of the stenosis in the peripheral region such that $\left[\bar\delta_p/\bar R_0\right]<<1$, $\bar R_1(\bar z)$ is the radius of the artery in the stenosed core region, β is the ratio of the central core radius to the normal artery radius, $\beta\bar R_0$ is the radius of the core region of the normal artery, $\bar\delta_C$ is the maximum height of the stenosis in the core region such that $\left[\bar\delta_C/\bar R_0\right]<<1$; $\bar\tau_y$ is the yield stress; θ is the non-dimensional yield stress; $\bar\rho_H$, $\bar\rho_N$ are the densities of the Herschel-Bulkley fluid and Newtonian fluid; $\bar\mu_0 = \bar\mu_H\left(2/\bar q_0\bar R_0\right)^{n-1}$ is the typical viscosity coefficient having the dimension as

that of the Newtonian fluid's viscosity, $\overline{q}_0$ is the negative of the pressure gradient in the normal artery; $\overline{Q}$ is the volume flow rate.

3. Method of solution

When we non-dimensionalize the constitutive equations, α_H^2 and α_N^2 occur naturally and these are time dependent and hence, it is more appropriate to expand the Eqs. (1)~(5) in perturbation series about α_H^2 and α_N^2. Let us expand u_p in powers of $\varepsilon_H\left(=\alpha_H^2\right)$ as below

$$u_p(z,t)=u_{op}(z,t)+\varepsilon_H u_{1p}(z,t)+\ldots\ldots\ldots \tag{11}$$

Similarly, one can expand u_H, u_N, τ_p, τ_H, τ_N, R_p in powers of ε_H and $\alpha_N\left(=\alpha_N^2\right)$ (where $\varepsilon_H << 1$ and $\varepsilon_N << 1$). Substituting the perturbation series expansions in Eqs. (1) and (3) and then equating the constant terms and ε_H terms, the resulting differential equations of the core region can be obtained as

$$\begin{aligned}
&\frac{\partial}{\partial r}\left(r\tau_{0H}\right)=2q(z)f(t)r\,,\quad \frac{\partial u_{0H}}{\partial t}=-\frac{2}{r}\frac{\partial}{\partial r}\left(r\tau_{1H}\right)\\
&-\frac{\partial u_{0H}}{\partial r}=2{\tau_{0H}}^{n-1}\left[\tau_{0H}-n\theta\right],\\
&-\frac{\partial u_{1H}}{\partial r}=2n{\tau_{0H}}^{n-2}\tau_{1H}\left[\tau_{0H}-(n-1)\theta\right]
\end{aligned} \tag{12}$$

Similarly, using the perturbation series expansions in Eqs. (2) and (5) and then equating the constant terms and ε_N terms, one can obtain the resulting differential equations of the peripheral region as

$$\begin{aligned}
&\frac{\partial}{\partial r}\left(r\tau_{0N}\right)=2q(z)f(t)r\,,\quad \frac{\partial u_{0N}}{\partial t}=-\frac{2}{r}\frac{\partial}{\partial r}\left(r\tau_{1N}\right)\\
&-\frac{\partial u_{0N}}{\partial r}=2\tau_{0N}\,,\quad -\frac{\partial u_{1N}}{\partial r}=2\tau_{1N}
\end{aligned} \tag{13}$$

Using the perturbation series expansions in Eq. (6) then equating the constant terms and ε_H and ε_N terms, one can get

$$\begin{aligned}
&\tau_{0p} \text{ and } \tau_{1p} \text{ are finite, } \frac{\partial u_{op}}{\partial r}=0, \text{ and } \frac{\partial u_{1p}}{\partial r}=0 \text{ at } r=0\\
&\tau_{0H}=\tau_{0N},\ \tau_{1H}=\tau_{1N},\ u_{oH}=u_{0N},\ u_{1H}=u_{1N} \text{ at } r=R_1(z)\\
&u_{0N}=0,\ u_{1N}=0 \text{ at } r=R
\end{aligned} \tag{14}$$

On solving the Eqs. (12) and (13) for the unknowns u_{0p}, u_{1p}, u_{0H}, u_{1H}, τ_{0p}, τ_{1p} τ_{0H}, τ_{1H}, u_{0N}, u_{1N}, τ_{0N} and τ_{1N}, using Eq. (14), one can obtain,

$$\begin{aligned}
&\tau_{0p}=q(z)f(t)R_{0p},\ \tau_{0H}=q(z)f(t)r\,,\\
&\tau_{0N}=q(z)f(t)r
\end{aligned} \tag{15}$$

$$u_{0N}=q(z)f(t)R^2\left[1-\xi^2\right] \tag{16}$$

$$\begin{aligned}
u_{0H}=\;&q(z)f(t)R^2\left\{1-\Omega^2\right\}+2\left[q(z)f(t)R_1\right]^n\times\\
&R_1\left[\left(1/(n+1)\right)\left\{1-\psi^{n+1}\right\}-\zeta\left\{1-\psi^n\right\}\right]
\end{aligned} \tag{17}$$

$$\begin{aligned}
u_{0p}=\;&q(z)f(t)R^2\left\{1-\Omega^2\right\}+2\left[q(z)f(t)R_1\right]^n\times\\
&R_1\left[\left(1/(n+1)\right)\left\{1-\chi^{n+1}\right\}-\zeta\left\{1-\varphi^n\right\}\right]
\end{aligned} \tag{18}$$

$$\begin{aligned}
\tau_{1p}=\;&-(1/4)\frac{1}{4}q(z)f(t)BR^3\sigma\left\{1-\Omega^2\right\}-\left[q(z)f(t)R_1\right]^n\times\\
&BR_1{}^2\left[\left(n/2(n+1)\right)\zeta-\left(\left(n^2-1\right)/2\right)\zeta^2\right.\\
&\left.-\left(n/2(n+1)\right)\zeta^{n+2}\right]
\end{aligned} \tag{19}$$

$$\begin{aligned}
\tau_{1H}=\;&-(1/4)q(z)f(t)BR^3\xi\left\{1-\Omega^2\right\}-\left[q(z)f(t)R_1\right]^n\times\\
&BR_1^2\left[\left(n/(n+1)(n+3)\right)\left\{\left((n+3)/2\right)\psi-\psi^{n+2}\right\}\right.\\
&-\left(\left(n-1\right)/n+2\right)\zeta\left\{\left((n+2)/2\right)\psi-\psi^{n+1}\right\}\\
&\left.-\left(3\left(n^2+2n-2\right)/2(n+2)(n+3)\right)\zeta^{n+3}\lambda\right]
\end{aligned} \tag{20}$$

$$\begin{aligned}
\tau_{1N}=\;&-q(z)f(t)BR^2R_1\times\\
&\left[(1/4)\psi-(1/8)\Omega^2\lambda-(1/8)\Omega^2\psi^3\right]\\
&-\left[q(z)f(t)R_1\right]^n BR_1^2\times\\
&\left[\left(n/2(n+3)\right)\lambda-\left(n(n-1)/2(n+2)\right)\zeta\lambda\right.\\
&\left.-\left(3\left(n^2+2n-2\right)/2(n+2)(n+3)\right)\zeta^{n+3}\lambda\right]
\end{aligned} \tag{21}$$

$$\begin{aligned}
u_{1N}=\;&-2q(z)f(t)BR^3R_1\times\\
&\left[(1/8)\eta\left\{1-\xi^2\right\}-(1/8)\Omega^3\log\nabla-(1/32)\eta\left\{1-\xi^4\right\}\right]\\
&-\left[q(z)f(t)R_1\right]^n BR_1^3\log\nabla\times\\
&\left[\left(n/2(n+3)\right)-\left(n(n-1)/2(n+2)\right)\zeta\right.\\
&\left.-\left(3\left(n^2+2n-2\right)/2(n+2)(n+3)\right)\zeta^{n+3}\right]
\end{aligned} \tag{22}$$

$$\begin{aligned}
u_{1H}=\;&-2q(z)f(t)BR^3R_1\times\\
&\left[(3/32)\eta-(1/8)\Omega+(1/32)\Omega^3+(1/8)\Omega^3\log\Omega\right]
\end{aligned}$$

$$
\begin{aligned}
&+2\left[q(z)f(t)R_1\right]^n BR_1^3\log\Omega\times\\
&\quad\left[\left(n/2(n+3)\right)-\left(n(n-1)/2(n+2)\right)\zeta\right.\\
&\quad\left.-\left(3\left(n^2+2n-2\right)/2(n+2)(n+3)\right)\zeta^{n+3}\right]\\
&-n\left[q(z)f(t)R_1\right]^n BR_1R^2\left\{1-\Omega^2\right\}\times\\
&\quad\left[\left(1/2(n+1)\right)\left\{1-\psi^{n+1}\right\}-\left((n-1)/2n\right)\zeta\left\{1-\psi^n\right\}\right]\\
&-2n\left[q(z)f(t)R_1\right]^{2n-1}BR_1^3\times\\
&\quad\left[\left(n/2(n+1)^2\right)\left\{1-\psi^{n+1}\right\}\right.\\
&\quad\left.-\left((n-1)/2(n+1)\right)\zeta\left\{1-\psi^n\right\}\right.\\
&-\left(n/2(n+1)^2(n+3)\right)\left\{1-\psi^{2n+2}\right\}\\
&+\left((n-1)\left(2n^2+6n+3\right)/(n+1)(n+2)(n+3)(2n+1)\right)\times\\
&\quad\zeta\left\{1-\psi^{2n+1}\right\}\\
&-\left((n-1)/2(n+1)\right)\zeta\left\{1-\psi^{n+1}\right\}\\
&+\left((n-1)^2/2n\right)\zeta^2\left\{1-\psi^n\right\}\\
&-\left((n-1)^2/2n(n+2)\right)\zeta^2\left\{1-\psi^{2n}\right\}\\
&-\left(3\left(n^2+2n-2\right)/2(n-1)(n+2)(n+3)\right)\times\\
&\quad\zeta^{n+3}\left\{1-\psi^{n-1}\right\}\\
&+\left(3(n-1)\left(n^2+2n-2\right)/2(n-2)(n+2)(n+3)\right)\times\\
&\quad\zeta^{n+4}\left\{1-\psi^{n-2}\right\}\Big]
\end{aligned}
\tag{23}
$$

$$
\begin{aligned}
u_{1p}&=-2q(z)f(t)BR^3R_1\times\\
&\quad\left[(3/32)\eta-(1/8)\Omega+(1/32)\Omega^3+(1/8)\Omega^3\log\Omega\right]\\
&+2\left[q(z)f(t)R_1\right]^n BR_1^3\log\Omega\times\\
&\quad\left[\left(n/2(n+3)\right)-\left(n(n-1)/2(n+2)\right)\zeta\right.\\
&\quad\left.-\left(3\left(n^2+2n-2\right)/2(n+2)(n+3)\right)\zeta^{n+3}\right]\\
&-n\left[q(z)f(t)R_1\right]^n BR_1R^2\left\{1-\Omega^2\right\}\times\\
&\quad\left[\left(1/2(n+1)\right)\left\{1-\zeta^{n+1}\right\}-\left((n-1)/2n\right)\zeta\left\{1-\zeta^n\right\}\right]\\
&-2n\left[q(z)f(t)R_1\right]^{2n-1}\times\\
&BR_1^3\left[\left(n/2(n+1)^2\right)\left\{1-\zeta^{n+1}\right\}\right.\\
&-\left((n-1)/2(n+1)\right)\zeta\left\{1-\zeta^n\right\}\\
&-\left(n/2(n+1)^2(n+3)\right)\left\{1-\zeta^{2n+2}\right\}\\
&+\left((n-1)\left(2n^2+6n+3\right)/(n+1)(n+2)(n+3)(2n+1)\right)\times\\
&\quad\zeta\left\{1-\zeta^{2n+1}\right\}\\
&-\left((n-1)/2(n+1)\right)\zeta\left\{1-\zeta^{n+1}\right\}\\
&+\left((n-1)^2/2n\right)\zeta^2\left\{1-\zeta^n\right\}\\
&-\left((n-1)^2/2n(n+2)\right)\zeta^2\left\{1-\zeta^{2n}\right\}\\
&-\left(3\left(n^2+2n-2\right)/2(n-1)(n+2)(n+3)\right)\zeta^{n+3}\times\\
&\quad\left\{1-\zeta^{n-1}\right\}\\
&+\left(3(n-1)\left(n^2+2n-2\right)/2(n-2)(n+2)(n+3)\right)\times\\
&\quad\zeta^{n+4}\left\{1-\zeta^{n-2}\right\}\Big]
\end{aligned}
\tag{24}
$$

where $k^2=r\big|_{\tau_{0p}=\theta}=R_{0p}=\theta/[q(z)f(t)]$, B=[1/f(t)] $df(t)/dt$, $\xi=(r/R)$, $\psi=(r/R_1)$, $\Omega=(R_1/R)$, $\eta=(R/R_1)$, $\chi=(R_{0p}/R_1)$, $\sigma=(k^2/R)$, $\zeta=(k^2/R_1)$, $\lambda=(R_1/r)$, . $\nabla=(R/r)$.

The expression for wall shear stress τ_w can be obtained by evaluating τ_N at $r=R$ and is given below.

$$
\begin{aligned}
\tau_w&=\left(\tau_{0N}+\alpha_N{}^2\tau_{1N}\right)_{r=R}=\tau_{0w}+\alpha_N{}^2\tau_{1w}\\
&=\left[q(z)f(t)R\right]\\
&\quad+\alpha_N{}^2\left\{-(1/8)q(z)f(t)BR^3\left[1-\Omega^4\right]\right\}\\
&+\alpha_N{}^2\left\{-\left(\left[q(z)f(t)R_1\right]^n/2(n+2)(n+3)\right)BR_1{}^2\Omega\times\right.\\
&\quad\left[n(n+2)-n(n-1)(n+3)\zeta\right.\\
&\quad\left.-3\left(n^2+2n-2\right)\zeta^{n+3}\right]
\end{aligned}
\tag{25}
$$

From Eq. (9), (16)-(18) and (22)-(24), the volume flow rate is calculated and is given by

$$
\begin{aligned}
Q&=4\int_0^{R_{0p}}\left(u_{0p}+\alpha_H^2u_{1p}\right)rdr+4\int_{R_{0p}}^{R_1}\left(u_{\right.}\\
&\quad+4\int_{R_1}^{R}\left(u_{0N}+\alpha_N^2u_{1N}\right)rdr\\
&=4q(z)f(t)R^4\left\{1-\Omega^2\right\}\left[\zeta^2+(1/4)\left\{1-\Omega^2\right\}\right]\\
&+4\left(\left[q(z)f(t)R_1\right]^n R_1^3/(n+2)(n+3)\right)\\
&\left[(n+2)-n(n+3)\zeta+\left(n^2+2n-2\right)\zeta^{n+3}\right]\\
&+4\alpha_H{}^2\left[-q(z)f(t)BR^3R_1{}^3\times\right.\\
&\quad\left\{(3/32)\eta-(1/8)\Omega+(1/32)\Omega^3+(1/8)\Omega^3\log\Omega\right\}\\
&+\left[q(z)f(t)R_1\right]^n B\quad R_1{}^5\log\Omega\times\\
&\quad\left\{\left(n/2(n+3)\right)-\left(n(n-1)/2(n+2)\right)\zeta\right.\\
&\quad\left.-\left(3\left(n^2+2n-2\right)/2(n+2)(n+3)\right)\zeta^{n+3}\right\}
\end{aligned}
$$

$$
\begin{aligned}
&-n\left[q(z)f(t)R_1\right]^n B\ \ R^2R_1^3\left\{1-\Omega^2\right\}\times\\
&\quad\left\{\left(1/4(n+3)\right)-\left((n-1)/4(n+2)\right)\zeta\right.\\
&\quad\left.+\left(\left(n^2+n-5\right)/4(n+2)(n+3)\right)\zeta^{n+3}\right\}\\
&-n\left[q(z)f(t)R_1\right]^{2n-1}BR_1^5\left\{\left(n/2(n+2)(n+3)\right)\right.\\
&-\left(n(n-1)\left(4n^2+12n+5\right)/(n+2)(n+3)\times\right.\\
&\quad\left.(2n+1)(2n+3)\right)\zeta\\
&+\left(n\left(n-1^2\right)/2(n+1)(n+2)\right)\zeta^2\\
&+\left(\left(n^3-2n^2-11n+6\right)/2(n+1)(n+2)(n+3)\right)\zeta^{n+3}\\
&-\left(\left(n-1\right)\left(n^3-2n^211n+6\right)/2n(n+2)(n+3)\right)\zeta^{n+4}\\
&-\left(\left(4n^5+14n^4-8n^3-45n^2-3n+18\right)/\right.\\
&\quad\left.2n(n+1)(n+2)(n+3)(2n+3)\right)\zeta^{2n+4}\Big\}\Big]\\
&+4\alpha_N{}^2\left[-q(z)f(t)BR^5R_1\right.\\
&\quad\left\{(1/24)\eta-(3/32)\Omega+(5/96)\Omega^5\right.\\
&\quad\left.-(1/8)\Omega^3\left(\log R_1\right)\left(1-\Omega^2\right)\right\}\\
&-\left[q(z)f(t)R_1\right]^n BR^2R_1^3\left\{1-\Omega^2\right\}(1+2\log R_1)\times\\
&\left\{\left(n/4(n+3)\right)-\left(n(n-1)/4(n+2)\right)\zeta\right.\\
&\left.-\left(3\left(n^2+2n-2\right)/4(n+2)(n+3)\right)\zeta^{n+3}\right\}
\end{aligned}
\tag{26}
$$

The second approximation to plug core radius R_{1p} can be obtained by neglecting the terms with ε_H^2 and higher powers of ε_H in the perturbation series expansion of R_P in the following manner. The shear stress $\tau_H=\tau_{0H}+\alpha_H{}^2\tau_{1H}$ at $r=R_p$ is given by

$$
\left|\tau_{0H}+\alpha_H{}^2\tau_{1H}\right|_{r=R_p}=\theta \tag{27}
$$

Using the Taylor's series of τ_{0H} and τ_{1H} about R_{0p} and using $\tau_{0H}|_{r=R0p}=\theta$, we get

$$
R_{1p}=\left[1/q(z)f(t)\right]\left[-\tau_{1H}\Big|_{r=R_{0p}}\right] \tag{28}
$$

Using the Eqs. (15), (20) and (28) in the perturbation series expansion of R_p ,the expression for plug core radius can be obtained as

$$
\begin{aligned}
R_p=&\,k^2+\left(B\alpha_H^2R^3/4\right)\sigma\left\{1-\Omega^2\right\}\\
&+\left(nB\alpha_H^2R_1^3/2(n+1)\right)\left[q(z)f(t)R_1\right]^{n-1}\times\\
&\left\{\zeta-\left(\left(n^2-1\right)/n\right)\zeta^2-\zeta^{n+2}\right\}
\end{aligned}
\tag{29}
$$

The resistance to flow in the artery is given by

$$
\Lambda=\left[q(z)f(t)\right]/Q \tag{30}
$$

When $R_1=R$, the present model reduces to the single fluid model (Herschel-Bulkley fluid model) and in such case, the expressions obtained in the present model for velocity u_H, shear stress τ_H, wall shear stress τ_w, flow rate Q and plug core radius R_p are in good agreement with those of Sankar and Hemalatha (2006).

4. Results and discussion

The objective of the present model is to understand and bring out the salient features of the effects of the pulsatility of the flow, non-Newtonian nature of blood, peripheral layer and stenosis size on various flow quantities in a blood flow through a stenosed artery when blood is represented by a two-fluid model with a core region of suspension of red cells represented by the Herschel-Bulkley fluid and a peripheral layer of plasma assumed as the Newtonian fluid. Some flow quantities of the single fluid model, which is obtained as a deduction from the present study, are compared with Sankar and Hemalatha (2006).

It is observed that the typical value of the power law index n for blood flow models is taken to lie between 0.9 and 1.1 and we have used the typical value of n to be 0.95 for n < 1 and 1.05 for n > 1 (Sankar and Hemalatha, 2006). Since, the value of yield stress is 0.04 dyne/cm^2 for blood at a haematocrit of 40 (Merrill, 1969). In diseased state, the value of yield stress is quite high (almost five times) (Chaturani and Ponnalagar Samy, 1985). The range 0.1 to 0.3 is used for the non-dimensional yield stress θ in this study. To compare the present results with the earlier results, we have used the yield stress value as 0.01 and 0.04. Though the range of the amplitude A is from 0 to 1, we use the range from 0.1 to 0.5 to pronounce its effect.

The ratio $\alpha(=\alpha_N/\alpha_H)$ between the pulsatile Reynolds numbers of the Newtonian fluid and Herschel-Bulkley (H-B) fluid is called pulsatile Reynolds number ratio. Though the pulsatile Reynolds number

ratio α ranges from 0 to 1, it is appropriate to assume its value as 0.5 (Srivastava and Saxena, 1994). Though the pulsatile Reynolds number α_H of the Herschel-Bulkley fluid ranges from 0 to 1 (Sankar and Hemalatha, 2006), the values 0.5 and 0.25 are used to analyze its effect on the flow quantities. The value of the ratio β of central core radius $\beta\overline{R}_0$ to the normal artery radius $\overline{R}_0$ in the unobstructed artery is generally taken as 0.95 (Srivastava and Saxena, 1994). Following Shukla et al. (1980a), relations $R_1 = \beta R$ and $\delta_c = \beta\delta_p$ are used to estimate R_1 and δ_c. The maximum thickness of the stenosis in the peripheral region δ_P is taken in the range 0.1 to 0.15 (Srivastava and Saxena, 1994). But, to compare the present results with those of Sankar and Hemalatha (2006) for single fluid model, value 0.2 is used for δ_c. When $\beta = 1$, the present model reduced to single fluid model (Newtonian fluid model or Herschel-Bulkley fluid model).

It is observed that in Eq. (65), $f(t)$, R and θ are known and Q and $q(z)$ are the unknowns to be determined. A careful analysis of Eq. (65) reveals the fact that $q(z)$ is the pressure gradient of the steady flow. Thus, if steady flow is assumed, then Eq. (65) can be solved for $q(z)$ (Chaturani and Ponnalagar Samy, 1986; Sankar and Hemalatha, 2006). For steady flow, Eq. (65) reduces to

$$\begin{aligned}&\left(R^2 - R_1^2\right)\left[4\theta^2\eta^2 + \left(R^2 - R_1^2\right)\right]y^3 \\ &+\left[4/(n+2)(n+3)\right]\times \\ &\left[(n+2)(R_1 y)^{n+3} - n(n+3)\theta(R_1 y)^{n+2}\right. \\ &\left.+\left(n^2+2n-2\right)\theta^{n+3}\right] - Q_S y^3 = 0\end{aligned} \tag{31}$$

where $y = q(z)$ and Q_S is the steady state flow rate. Eq. (31) can be solved for x numerically for a given value of n, Q_S and θ. Eq. (31) has been solved numerically for x using Newton-Raphson method with variation in the axial direction and yield stress with $\beta = 0.95$ and $\delta_p = 0.1$. Throughout the analysis, the steady flow rate Q_S value is taken as 1.0.

4.1 Pressure gradient

The values of the pressure gradient $q(z)$ for the two fluid model for different values of the axial distance z and yield stress θ with $n = 0.95$ and $n = 1.05$ are given in Tables 1 and 2 respectively. We have assumed that the stenotic region is located between $z = 4$ and $z = 6$ and is of length 2. Since, the values of the pressure gradient $q(z)$ are symmetric about $z = 5$, the middle of the stenosis, the values are tabulated only between $z = 4$ and $z = 5$. It is clearer that the pressure gradient increases for increasing values of the yield stress θ for a given value of R. From Tables 1 and 2, it has been observed that the pressure gradient $q(z)$ values are higher when $n = 1.05$ than the one for $n = 0.95$ from $z = 4$ to $z = 4.3$, whereas from $z = 4.3$ to $z = 5$ the behavior is reversed. The values of the pressure gradient for the single fluid model (when $\beta = 1$) with $n = 0.95$ are in good agreement with the values in Table 1 of Sankar and Hemalatha (2006). In the case of single-fluid model of Herschel-Bulkley

Table 1. Variation of pressure gradient with axial distance with with $n = \beta = 0.95$ and $\delta_P = 0.1$.

z \ θ	0.01	0.05	0.1	0.3
4	1.2233	1.2782	1.3442	1.5783
4.1	1.2358	1.2909	1.357	1.5916
4.2	1.2731	1.3286	1.3952	1.6311
4.3	1.334	1.3901	1.4574	1.6955
4.4	1.416	1.4728	1.5411	1.782
4.5	1.5143	1.572	1.6413	1.8854
4.6	1.6211	1.6798	1.7502	1.9975
4.7	1.7257	1.7852	1.8566	2.1069
4.8	1.8146	1.8749	1.947	2.1998
4.9	1.8748	1.9355	2.0082	2.2624
5	1.8961	1.957	2.0298	2.2846

Table 2. Variation of pressure gradient with axial distance with $n = 1.05$, $\delta_P = 0.1$ and $\beta = 0.95$.

Z \ θ	0.01	0.05	0.1	0.3
4	1.236	1.2908	1.3572	1.5979
4.1	1.2478	1.3027	1.3692	1.6104
4.2	1.2827	1.338	1.4049	1.6476
4.3	1.3395	1.3954	1.4631	1.7081
4.4	1.4157	1.4724	1.541	1.781
4.5	1.5067	1.5643	1.6339	1.8853
4.6	1.6051	1.6636	1.7343	1.9892
4.7	1.7009	1.7603	1.832	2.0901
4.8	1.7821	1.8422	1.9147	2.1754
4.9	1.8368	1.8973	1.9704	2.2328
5	1.8561	1.9168	1.9901	2.2531

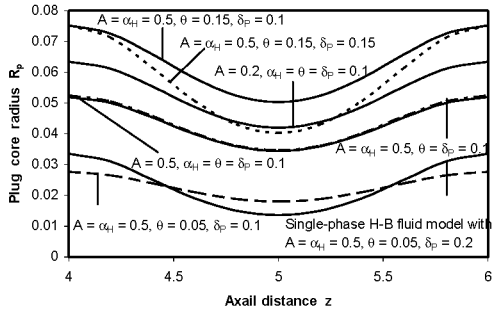

Fig. 2. Variation of plug core radius with axial direction for different values of A, α_H, θ and δ_P with $n = \beta = 0.95$.

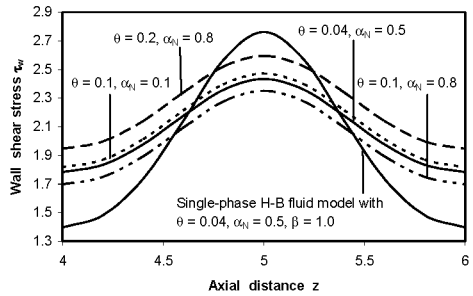

Fig. 3. Variation of wall shear stress with axial distance for different values θ and α_N with $t = 45°$, $n = \beta = 0.95$, $A = 0.5$ and $\delta_P = 0.1$.

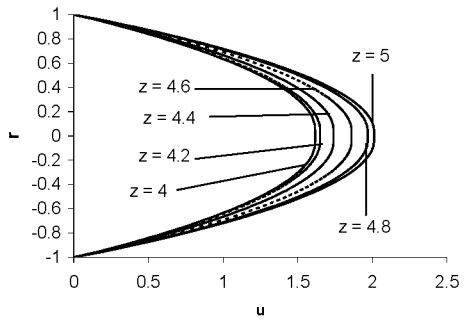

Fig. 4. Velocity distribution at different locations of the stenosis with $n = \beta = 0.95$, $\alpha = \alpha_H = 0.5$, $\theta = \delta_P = 0.1$, $A = 0.5$ and $t = 45°$.

fluid with $\delta_c = 0.2$ (Sankar and Hemalatha, 2006), the pressure gradient $q(z)$ values are higher when $n = 1.05$ than the one for $n = 0.95$ from $z = 4$ to $z = 4.5$, whereas from $z = 4.5$ to $z = 5$ the behavior is reversed. It is of interest to note that the above change in the pressure gradient in the axial direction occurred due to the presence of the peripheral layer. Since, there is only a slight difference in the values of the pressure gradient for $n = 0.95$ and $n = 1.05$, we often use the value 0.95 for the power law index n in the analysis of the other flow quantities.

4.2 Plug core radius

The variation of plug core radius (R_p) with axial distance for different values of the amplitude A, stenosis thickness δ_p, yield stress θ and pulsatile Reynolds number of the Herschel-Bulkley (H-B) fluid α_H with $n = \beta = 0.95$, and $t = 60°$ is shown in Fig. 2. It is noted that the plug core radius decreases as the axial variable z varies from 4 to 5 and it increases as z varies from 5 to 6. It is further observed that for the given values of δ_p, θ and α_H, the plug core radius decreases with the increase of the amplitude A and the same behavior is noted as the peripheral layer stenosis thickness or pulsatile Reynolds number α_H of the Herschel-Bulkley fluid increases when the other parameters held constant. Further, it is noticed that the plug core radius increases with the increase of the yield stress θ while the other parameters are kept as invariables. It is of interest to observe that the plug core radius for the single-phase Herschel-Bulkley fluid model is in good agreement with Fig. 4 of Sankar and Hemalatha (2006). Further, it is noticed that the plug core radius for the two-phase Herschel-Bulkley fluid model is lower than that of the single-phase Herschel-Bulkley fluid model when the axial variable z lies between 4 and 4.5 and also between 5.5 and 6. The behavior is reversed when the axial variable z lies between 4.5 and 5.5. It is also found that the width of the plug core region is smaller for the two-phase model than that of the single-phase model. Figure 4 depicts the effects of stenosis height, pulsatilty and amplitude of the flow on the plug core radius of the blood vessels.

4.3 Wall shear stress

The variation of wall shear stress in the axial direction for different values of yield stress θ and pulsatile Reynolds number α_N of the Newtonian fluid with $t = 45°$, $n = \beta = 0.95$, $A = 0.5$ and $\delta_p = 0.1$ is plotted in Fig. 3. It is found that the wall shear stress increases as the axial variable z increases from 4 to 5 and then it decreases symmetrically as z increases further from 5 to 6. For a given value of the pulsatile Reynolds number α_N, the wall shear stress increases considerably with the increase in the values of the yield stress θ when the other parameters held constant. Also, it is noticed that for a given value of the yield stress θ and increasing values of the pulsatile

Reynolds number α_N, the wall shear stress decreases slightly while the other parameters are kept as invariables. It is of interest to note that the plot for the single-phase Herschel-Bulkley fluid model is in good agreement with Fig. 8 of Sankar and Hemalatha (2006). Further, it is found that the wall shear for the two-phase Herschel-Bulkley fluid model is higher than those of the single-phase Herschel-Bulkley fluid model when the axial variable z lies between 4 and 4.5 and also between 5.5 and 6, and, the behaviour is reversed when the axial variable z lies between 4.5 and 5.5. Figure 3 shows the effects of pulsatility of the blood flow and non-Newtonian effects of the blood on the wall shear stress of the two-fluid model.

4.4 Velocity distribution

The velocity distributions in the radial direction at different locations of the stenosis with $n = \beta = 0.95$, $\alpha = \alpha_H = 0.5$, A = 0.5, $\theta = \delta_p = 0.1$ and $t = 45°$ are shown in Fig. 4. One can easily notice the plug flow around the tube axis in Fig. 8. Also, it is found that the velocity increases with the increases with the axial distance from z = 4 to z = 6 (in the stenosed region).It is noted that the velocity is maximum at the middle of the stenosis and minimum at the unobstructed position of the tube (z = 4) and the behavior is reversed from z = 5 to z = 6. This figure shows the effects of stenosis on the velocity of the two-fluid model.

4.5 Resistance to flow

The variation of resistance to flow in a time cycle for different values of θ, δ_P and β with n = 0.95, α = α = 0.25 and A = 0.2 is sketched in Fig. 5. It is found that the resistance to flow decreases as time t (in degrees) increases from 0° to 90° and then it increases as t increases from 90° to 270° and then again it decreases as t increases further from 270° to 360°. The resistance to flow is minimum at 90° and maximum at 270°. Further, it is noticed that for the fixed values of β and with the increasing values of the stenosis thickness δ_P or yield stress θ, the resistance to flow increases significantly. It is observed that for the fixed values of θ and δ_P and, with the increasing values of the ratio β (ratio between the central core radius to the normal artery radius), the resistance to flow decreases considerably. It means that the resistance to flow decreases significantly with the increase of the cell-free peripheral layer thickness. This figure depicts the effects of stenosis, peripheral layer thickness and yield stress on resistance to flow of the two-phase model of blood flow.

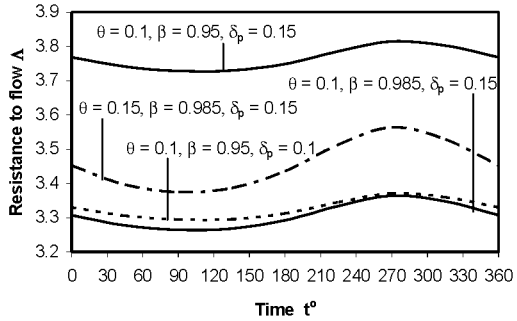

Fig. 5. Variation of resistance to flow in a time cycle for different values of β and δ_P with n = 0.95, α = α_H = 0.25 and A = 0.2.

Table 3. Magnitudes of the wall shear stress (τ_w) and resistance to flow (Λ) for two-fluid model and single-fluid for different stenosis sizes with $n = 0.95$, $\alpha = \alpha_H = 0.5$, $\beta = 0.99$, $A = 0.5$, $\theta = 0.1$ and t = 45°.

Stenosis size(δ_P)	Two-fluid model		Single-fluid model	
	τ_w	Λ	τ_w	Λ
0.025	1.677	4.85638	1.7392	4.91482
0.05	1.8058	5.11049	2.0313	5.48383
0.075	1.9495	5.39174	2.3993	6.19112
0.1	2.1102	5.70411	2.8696	7.08467
0.125	2.2907	6.05234	3.4798	8.23424
0.15	2.4939	6.44208	4.2856	9.74395

Table 4. Percentage of increase in the wall shear stress (τ_w) and resistance to flow (Λ) for two-fluid model and single-fluid over uniform diameter tube for different stenosis sizes with $n = 0.95$, $\alpha = \alpha_H = 0.5$, $\beta = 0.99$, $A = 0.5$, $\theta = 0.1$ and t = 45°.

Stenosis size(δ_P)	Two-fluid model		Single-fluid model	
	τ_w	Λ	τ_w	Λ
0.025	7.41	4.98	15.59	10.44
0.05	15.66	10.47	35	23.22
0.075	24.86	16.55	59.45	39.12
0.1	35.16	23.31	90.71	59.19
0.125	46.72	30.83	131.26	85.02
0.15	59.73	39.26	184.81	118.95

The wall shear stress (τ_w) and resistance to flow (Λ) are physiologically important flow quantities which play an important role in the formation of platelets (Karino and Goldsmith, 1977). High wall shear stress

not only damage the vessel wall and cause intimal thickening, but also activate platelets, cause platelet aggregation, and finally results in the formation of thrombus (Liu et al., 2004). The magnitudes of the wall shear stress (τ_w) and resistance to flow for the two-fluid and single-fluid Herschel-Bulkley fluid models for different stenosis sizes with $n = 0.95$, $\beta = 0.99$, $A = 0.5$, $\alpha = \alpha_H = 0.5$, $\theta = 0.1$ and $t = 45°$ are given in Table 3. It is found that the wall shear stress and resistance to flow for the two-fluid model is considerably less than that of the single-fluid model. The percentage of increase in the wall shear stress and resistance to flow for the two-fluid model and single fluid model over the uniform diameter tube(without stenosis) for different stenosis sizes with $n = 0.95$, $\beta = 0.99$, $A = 0.5$, $\alpha = \alpha_H = 0.5$, $\theta = 0.1$ and $t = 45°$ is given in Table 5. From Table 4, one can expect a marked increase in the flow of the two-fluid model, since, the percentage of increase in the resistance to flow and wall shear stress is considerably very low for the two-fluid model than that of the single-fluid model.

5. Conclusions

The results based on the perturbation analysis and the subsequent numerical evaluations indicate that the plug core radius and resistance to flow increase as the stenosis size δ_p increases while all other parameters held constant. It is found that the plug core radius decreases as the amplitude A increases when all other parameters held constant. The wall shear stress increases with the increase of yield stress while keeping the other parameters as invariables. It is observed that the velocity increases with the axial distance in the stenosed region of the tube upto the maximum projection of the stenosis (i.e. from z = 4 to z = 5) and the behavior is reversed if the height of the stenosis decreases (from z = 5 to z = 6). Thus, the results demonstrate that this model is capable of predicting the hydrodynamic features most interesting to physiologists. It is noted that the effects of the peripheral layer increases with the decrease of the blood vessel diameter in the two-fluid models. The two-fluid model analysis is better applied to vessels with diameter less than 0.2 mm where the non-Newtonian effects are expected to be significant (Srivastava, 1996).

Since, this study takes care of the pulsatility of the flow and also it incorporates the characteristics of the plug core region (which certainly exist in the case of non-Newtonian fluid flow in smaller diameter arteries), it is strongly felt that the present model may provide a better insight to the study of blood flow behavior in the stenosed arteries than the earlier models. Hence, the modeling of the blood flow through stenosed narrow arteries by a single-fluid model could not be appropriate. Also, the inaccurate predictions regarding the blood flow analysis may lead to wrong calculations. In view of these arguments, the present study could be useful for analyzing the blood flow in the diseased state. From this study, it is clear that the presence of the peripheral layer helps in the functioning of the diseased arterial system.

Acknowledgements

This work was supported by Inha Research Grant 2006.

Nomenclature

$\bar{r}$	:	Radial distance
r	:	Dimensionless radial distance
$\bar{z}$	:	Axial distance
z	:	Dimensionless axial distance
n	:	Power law index
$\bar{p}$	:	Pressure
p	:	Dimensionless pressure
$\bar{Q}$	:	Flow rate
Q	:	Dimensionless flow rate
$\bar{R}_0$	:	Radius of the normal artery
$\bar{R}(\bar{z})$	:	Radius of the artery in the stenosed peripheral region
$R(z)$	:	Dimensionless radius of the artery in the stenosed peripheral region
$\bar{R}_1(\bar{z})$	:	Radius of the artery in the stenosed core region
$R_1(z)$	:	Dimensionless radius of the artery in the stenosed core region
$\bar{R}_P$	:	Plug core radius
R_P	:	Dimensionless plug core radius
$\bar{u}_H$	:	Axial velocity of the Herschel-Bulkley fluid
u_H	:	Dimensionless axial velocity of the Herschel-Bulkley fluid
$\bar{u}_N$	:	Axial velocity of the Newtonian fluid
u_N	:	Dimensionless axial velocity of the Newtonian fluid

A : Amplitude of the flow
$\overline{q}(\overline{z})$: Steady state pressure gradient
$q(z)$: Dimensionless steady state pressure gradient
$\overline{q}_0$: Negative of the pressure gradient in the normal artery
$\overline{L}$: Length of the normal artery
$\overline{L}_0$: Length of the stenosis
L_0 : Dimensionless length of the stenosis
$\overline{d}$: Location of the stenosis
d : Dimensionless location of the stenosis
$\overline{t}$: Time
t : Dimensionless time

Greek letters

Δp : Dimensionless Pressure drop
Λ : Dimensionless resistance to flow
ϕ : Azimuthal angle
$\dot{\gamma}$: Shear rate
$\overline{\tau}_y$: Yield stress
θ : Dimensionless yield stress
$\overline{\tau}_H$: Shear stress for the Herschel-Bulkley fluid
τ_H : Dimensionless shear stress for the Herschel-Bulkley fluid
$\overline{\tau}_N$: Shear stress for the Newtonian fluid
τ_N : Dimensionless shear stress for the Newtonian fluid
τ_w : Dimensionless wall shear stress
$\overline{\rho}_H$: Density of the Herschel-Bulkley fluid
$\overline{\rho}_N$: Density of the Newtonian fluid
$\overline{\mu}_H$: Viscosity of the Herschel-Bulkley fluid
$\overline{\mu}_N$: Viscosity of the Newtonian fluid
α_H : Pulsatile Reynolds number of the Herschel-Bulkley fluid
α_N : Pulsatile Reynolds number of the Newtonian fluid
α : Ratio between the Reynolds numbers α_H and α_N
β : Ratio of the central core radius to the normal artery radius
$\overline{\delta}_C$: Maximum height of the stenosis in the core region
δ_C : Dimensionless maximum height of the stenosis in the core region
$\overline{\delta}_N$: Maximum height of the stenosis in the peripheral region
δ_P : Dimensionless maximum height of the stenosis in the peripheral region
$\overline{\omega}$: Angular frequency of the blood flow

Subscripts

w : Wall shear stress (used for τ)
C : Core region (used for $\overline{\delta}, \delta$)
P : Peripheral region (used for $\overline{\delta}, \delta$)
H : Herschel-Bulkley fluid (used for $\overline{u}, u, \overline{\tau}, \tau$)
N : Newtonian fluid (used for $\overline{u}, u, \overline{\tau}, \tau$)

References

Bakirtas, I., Antar, N., 2003, "Evolution Equations for Nonlinear Waves in a Tapered Elastic Tube Filled with a Viscous Fluid," *International Journal of Engineering. Science,* Vol. 41, pp. 1163~1176.

Bugliarello, G., Sevilla, J., 1970, "Velocity Distribution and Other Characteristics of Steady and Pulsatile Blood Flow in Fine Glass Tubes," *Biorheology*, Vol.7, pp. 85~ 107.

Chakravarthy, S., Mandal, P. K., 2000, "Two-Dimensional Blood Flow Through Tapered Arteries Under Stenotic Conditions," *International Journal of Non-Linear Mechanics,* Vol. 35, pp. 779~ 793.

Chaturani, P., Ponnalagar Samy, R., 1985, "A Study of Non-Newtonian Aspects of Blood Flow Through Stenosed Arteries and its Applications in Arterial Diseases," *Biorheology*, Vol. 22, pp. 521~ 531.

Chaturani, P., Ponnalagar Samy, R., 1986, "Pulsatile Flow of Casson's Fluid Through Stenosed Arteries with Applications to Blood Flow," *Biorheology*, Vol. pp. 23, 499~ 511.

Chiu, J. J., Wang, D. L., Chien, S., Skalak, R., Usami, S., 1998, "Effects of Disturbed Flow on Endothelial Cells," *ASME Journal of Biomechanical Engineering,* Vol. 120, pp. 2~ 8.

Cokelet, G. R., 1972, The Rheology of Human Blood, In: Fung, Y. C. (Eds), *Biomechanics,* Prentice-Hall, Englewood Cliffs, N. J., pp. 63~ 103.

Dash, R. K., Jayaraman, G., Metha, K. N., 1999, "Flow in a Catheterized Curved Artery with Mild Stenosis," *Journal of Biomechanics,* Vol. 32, pp. 49~ 61.

Iida, N., 1978, "Influence of Plasma Layer on Steady Blood Flow in Micro Vessels," *Japanese Journal of Applied Physics,* Vol. 17, pp. 203~ 214.

Kapur, J. N., 1992, *Mathematical Models and Mothods in Biology and Medicine,* Affiliated East – West Press Pvt. Ltd, New Delhi.

Karino, T., Goldsmith, H. L., 1977, "Flow Behavior of Blood Cells and Rigid Spheres in Annular Vortex," *Philosophical Transactions of the Royal Society,* Vol. B279, pp. 413~ 445.

Liepsch, D., Singh, M., Martin, L., 1992, "Experimental Analysis of the Influence of Stenotic Geometry on Steady Flow," *Biorheology*, Vol. 29, pp. 419~431.

Liu, G. T., Wang, X. J., Ai, B. Q., Liu, L. G., 2004, "Numerical Study of Pulsating Flow Through a Tapered Artery with Stenosis," *Chinese Journal of Physics,* Vol. 42, pp. 401~409.

Long, Q., Ku, X. Y., Ramnarine, K. V., Hoskins, P., 2001, "Numerical Investigations of Physiologically Realistic Pulsatile Flow Through Arterial Stenosis," *Journal of Biomechanics,* Vol. 34, pp. 1229~1242.

Mandal, P. K., 2005, "An Unsteady Analysis of Non-Newtonian Blood Flow Through Tapered Arteries with a Stenosis," *International Journal of Non-Linear Mechanics,* Vol. 40, pp. 151~164.

Marshall, I., Zhao, S., Papathanasopoulou, P., Hoskins, P., Xu, X. Y., 2004, "MRI and CFD Studies of Pulsatile Flow in Healthy and Stenosed Carotid Bifurcation Models," *Journal of Biomechanics,* Vol. 37, pp. 679~687.

Merrill, E. W., 1969, "Rheology of Blood," *Physiological Reviews,* Vol. 49, pp. 863~888.

Moayeri, M. S., Zendehbudi, G. R., 2003, "Effects of Elastic Property of the Wall on Flow Characteristics teristics Through Arterial Stenosis," *Journal of Biomechanics,* Vol. 36, pp. 525~535.

Pralhad, R. N., Schultz, D. H., 1988, "Two-Layered Blood Flow Through Stenosed Tubes for Different Diseases," *Biorheology,* Vol. 25, pp. 715~726.

Sankar D. S., Hemalatha, K., 2006, "Pulsatile Flow of Herschel-Bulkey Fluid Through Stenosed Arteries-A Mathematical Model," *International Journal of Non-Linear Mechanics,* Vol. 41, pp. 979~990.

Segers, P., Verdonck, P., 2000, "Role of Tapering in Arotic Wave Reflection: Hydraulic and Mathematical Model," *Journal of Biomechanics,* Vol. 33, pp. 299~306.

Shukla, J. B., Parihar, R. S., Gupta, S. P., 1980a, "Effects of Peripheral Layer Viscosity on Blood Flow Through the Artery with Mild Stenosis," *Bulletin of Mathematical Biology,* Vol. 42, pp. 797~805.

Shukla, J. B., Parihar, R. S., Rao, B. R. P., 1980b, "Effects of Stenosis on Non-Newtonian Flow of the Blood in an Artery," *Bulletin of Mathematical Biology,* Vol. 42, pp. 283~294.

Srivastava, V. P., Saxena, M., 1994, "Two-Layered Model of Casson Fluid Flow Through Stenotic Blood Vessels: Applications to the Cardiovascular System," *Journal of Biomechanics,* Vol. 27, pp. 921~928.

Srivastava, V. P., 1996, "Two-Phase Model of Blood Flow Through Stenosed Tubes in the Presence of a Peripheral Layer: Applications," *Journal of Biomechanics,* Vol. 29, pp. 1377~1382.

Tu, C., Deville, M., 1996, "Pulsatile Flow of Non-Newtonian Fluids Through Arterial Stenosis" *Journal of Biomechanics,* Vol. 29, pp. 899~908.